Electronic Supplementary Material (ESI) for New Journal of Chemistry.

Supporting Information

Utilization of Single Biomass-derived Micro-Mesoporous Carbon for Dual-Carbon Symmetric and Hybrid Sodium-ion Capacitors

Authors: Nagmani [a], Biraj Kanta Satpathy [b], Abhijeet Kumar Singh [a], Debabrata Pradhan [b,c] and Sreeraj Puravankara [a*]

Affiliations: [a] School of Energy Science & Engineering, Indian Institute of Technology Kharagpur, Kharagpur -721302, West Bengal, India

[b] School of Nanoscience and Technology, Indian Institute of Technology Kharagpur, Kharagpur -721302, West Bengal, India

[c] Materials Science Centre, Indian Institute of Technology Kharagpur, Kharagpur -721302, West Bengal, India

Corresponding author: **Dr. Sreeraj Puravankara**

School of Energy Science & Engineering, IIT Kharagpur,

Kharagpur -721302, West Bengal, India

Phone (Office) - +913222 260801

email: sreeraj@iitkgp.ac.in

ORCID ID

Nagmani: https://orcid.org/0000-0003-4618-4952

Biraj Kanta Satpathy: https://orcid.org/0000-0002-7639-024X

Abhijeet Kumar Singh: https://orcid.org/0009-0008-3383-5107

Sreeraj Puravankara: https://orcid.org/0000-0002-9238-0148

Debabrata Pradhan: https://orcid.org/0000-0003-3968-9610

Figures:

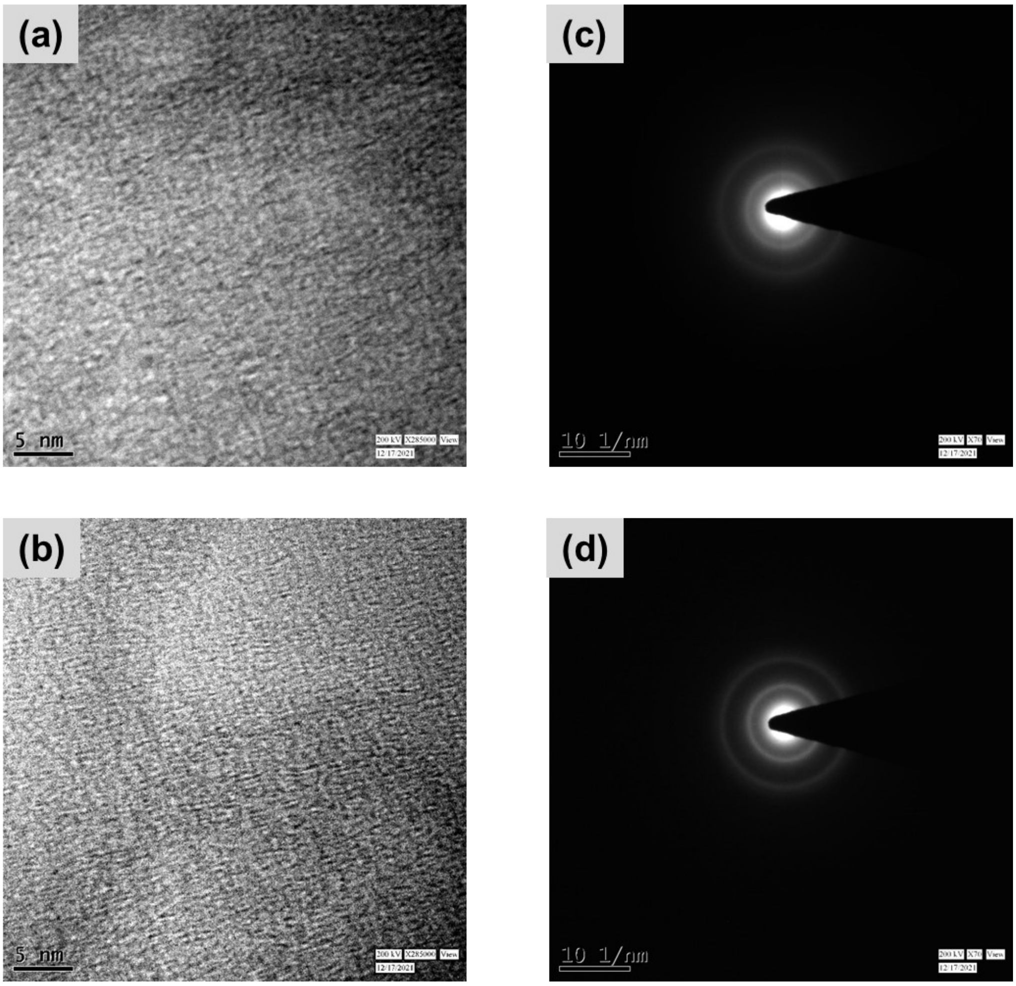

Figure S1: HR-TEM image showing the turbostratic curve (a) AJPC-M (b) AJPC-D.

SAED pattern showing the diffuse ring (c) AJPC-M, (d) AJPC-D.

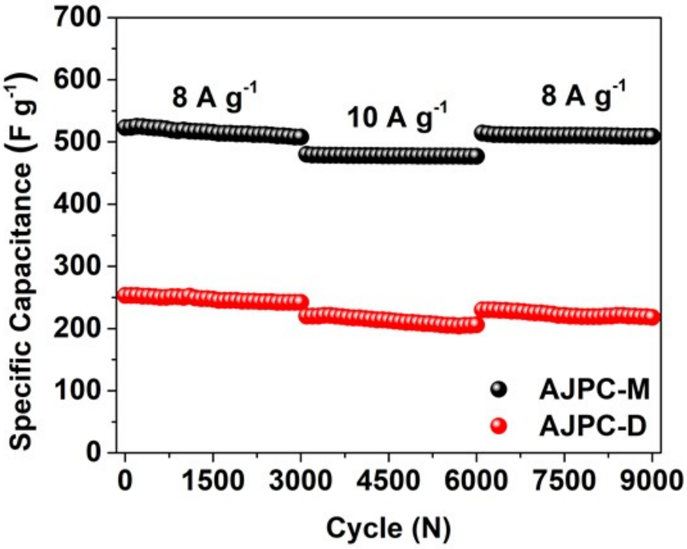

Figure S2: Long cyclic performance of AJPC-D and AJPC-M at the current density of 8 A g^{-1} and 10 A g^{-1}.

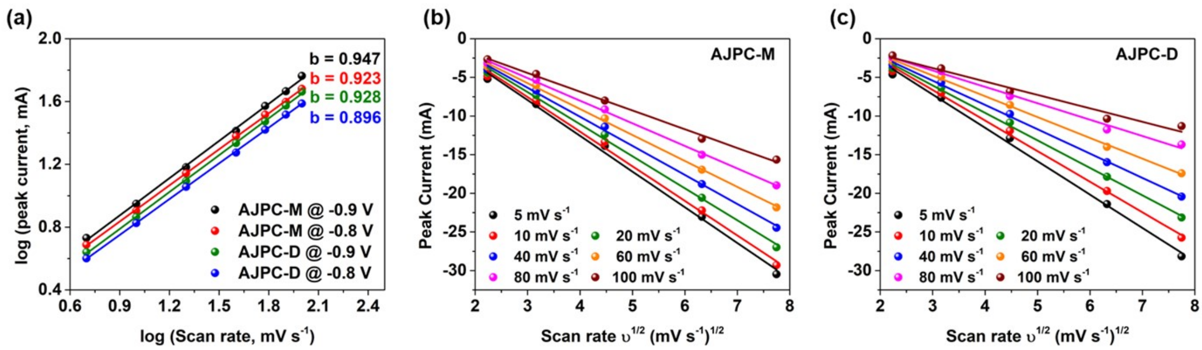

Figure S3: (a) Logarithmic plot for peak current vs. scan rate [log (i) and log (υ)].Plots for peak current and the square root of scan rate to calculate ions diffusion coefficient using Randles Sevcik equation in (b) AJPC-M, and (c) AJPC-D.

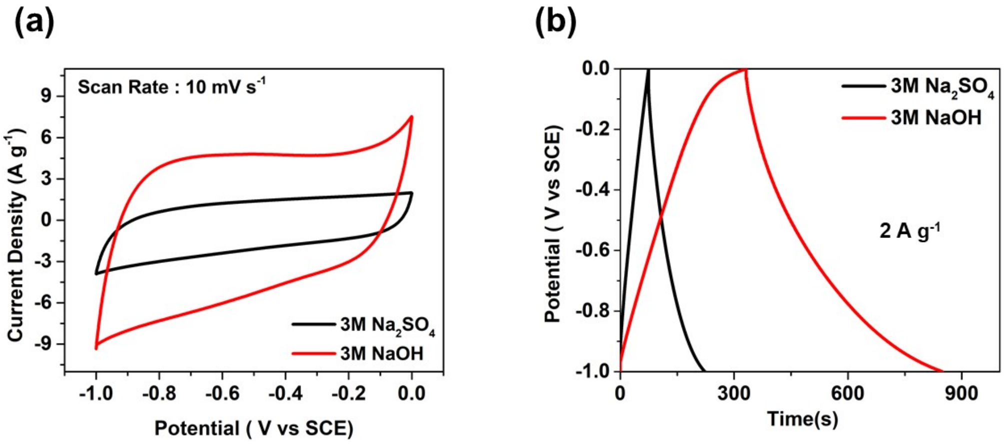

Figure S4: (a) CV curve (b) GCD curve at the current density of 2 A g^{-1} of AJPC-M using 3M NaOH (basic medium) and 3M Na_2SO_4 (neutral medium).

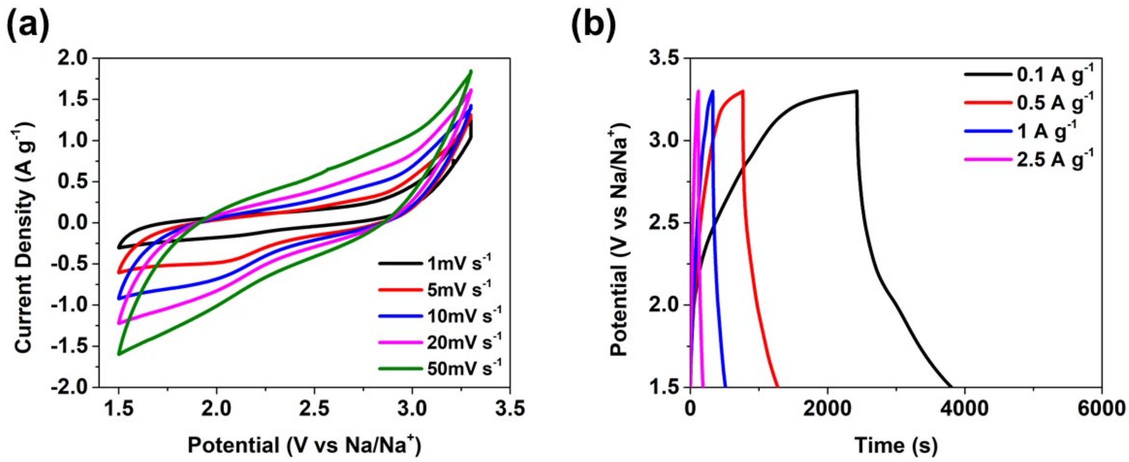

Figure S5: (a) CV curve at different scan rates for AJPC-M, (b) GCD profile for AJPC-D at different current densities.

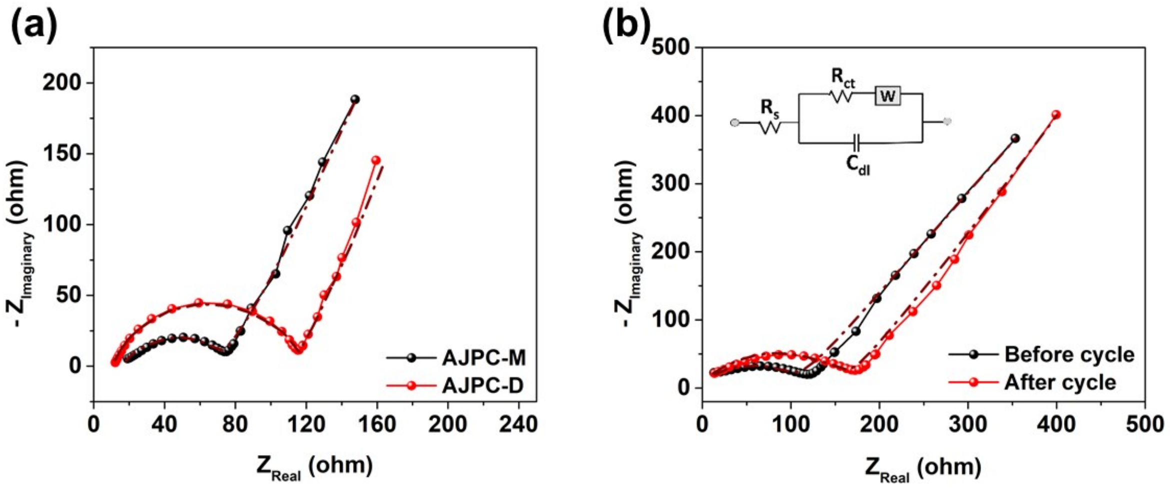

Figure S6: EIS spectra of AJPC-M and AJPC-D as cathode before cycling. (b) EIS spectra of SSIC (AJPC-M // AJPC-M) before and after the first cycle (inset: equivalent circuit).

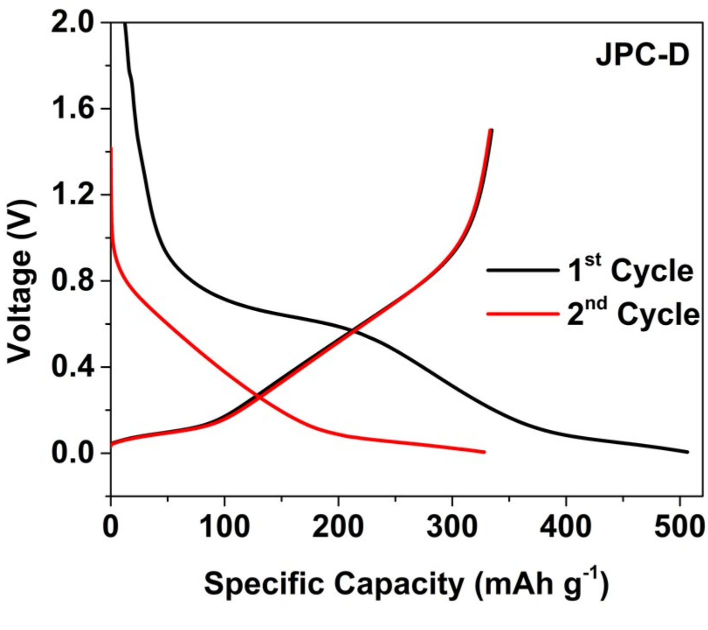

Figure S7: The GCD profile of hard carbon derived from jute via direct pyrolysis at a current density of 30 mA g^{-1}. (Reprinted (adapted) with permission.[1] Copyright 2022, American Chemical Society).

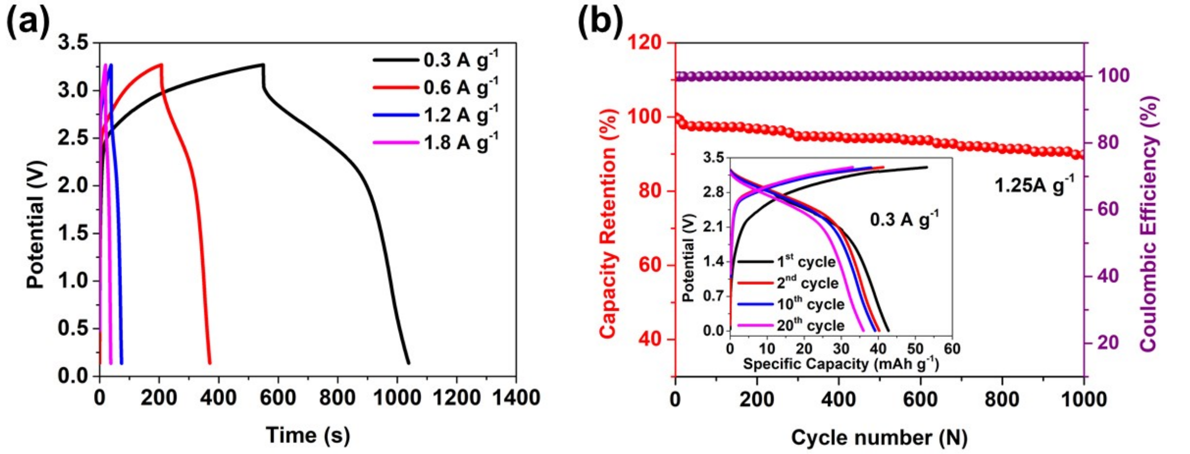

Figure S8: (a) The GCD profile of ASICs at different current densities, (b) long cyclic stability of ASICs at the current density of 1.25 A g^{-1} (inset: charge discharge profile at 0.3 A g^{-1})

Tables:

Table S1: Resistance values obtained from fitted EIS spectra of AJPC-electrode.

Electrode	**R_S (Ω)**	**R_{CT} (Ω)**	**R_{Total} (Ω)**
AJPC-D (Non-Aq)	1.43	0.65	2.08
AJPC-M (Non-Aq)	1.37	0.22	1.59
AJPC-D (Aq)	13	93	106
AJPC-M (Aq)	16	55	71

Table S2: A summary of SSICs device based on the biomass-derived carbon-based anode and cathode materials in an aqueous electrolyte system.

<table>
<tr><td>Material</td><td>ED</td><td>PD</td><td>Reference</td></tr>
<tr><td>Jute carbon</td><td>15.44</td><td>402.78</td><td>2</td></tr>
<tr><td>Jute sticks</td><td>20</td><td>500</td><td>3</td></tr>
<tr><td>Recycled jute</td><td>21</td><td>1820</td><td>4</td></tr>
<tr><td>Pomegranate</td><td>8.8</td><td>3950</td><td>5</td></tr>
<tr><td>Rice straw</td><td>9.31</td><td>500</td><td>6</td></tr>
<tr><td>Plastic (LDPE)</td><td>9.81</td><td>450</td><td>7</td></tr>
<tr><td>Algae microspheres</td><td>20</td><td>332</td><td>8</td></tr>
<tr><td>Cashew nut</td><td>11.2</td><td>400</td><td>9</td></tr>
<tr><td rowspan="2">AJPC-M</td><td>37.7</td><td>785</td><td rowspan="2">This Work</td></tr>
<tr><td>9.75</td><td>7895</td></tr>
</table>

Table S3: A summary of SICs device based on carbon-based anode and cathode materials in a non-aqueous electrolyte system.

Anode//cathode	**Carbon's Precursor**	**Maximum ED @ PD**	**Maximum PD @ ED**	**References**
Polyimide–Graphene//rGO	Polymide	55.5 @395	3400 @22.5	10
Hard carbon(coconut shell)//AC	Coconut shell	82@200	9000@20	11
Porous carbon//AC	Sucrose (STC-16)	61 @100	24000@12	12
C-CNT@Carbon Nanofiber//AC	Bacterial cellulose	59.1 @275	5500@38	13
PIGC//NBEG	Polyimide/graphene oxide	81@600	9500@55	14
Carbon sphere(CS)//AC(CS)	Fruit Juice	52.2@300	3000@18	15
S-NCNF//AC	Polyacrylonitrile	95@184	17000@24	16
EEG//AC	Commercial	90@2000	17500@17	17
Hard carbon //AC	Olive pit	100@345	9000@35	18
Brown- TiO_2 //AC	Commercial	68@625	7500@23	19
CNF// CNF	Lignin/PAN	68@172	2000@40	20
V_2O_3@MCNF//AC	Commercial	96@250	7680@76.8	21

References:

(1) Nagmani, Verma, P.; Puravankara, S. Jute-Fiber Precursor-Derived Low-Cost Sustainable Hard Carbon with Varying Micro/Mesoporosity and Distinct Storage Mechanisms for Sodium-Ion and Potassium-Ion Batteries. *Langmuir* **2022**, *38* (49). https://doi.org/10.1021/acs.langmuir.2c02575.

(2) Manasa, P.; Lei, Z. J.; Ran, F. Biomass Waste Derived Low Cost Activated Carbon from Carchorus Olitorius (Jute Fiber) as Sustainable and Novel Electrode Material. *Journal of Energy Storage*. **2020**, 101494. https://doi.org/10.1016/j.est.2020.101494.

(3) Shah, S. S.; Cevik, E.; Aziz, M. A.; Qahtan, T. F.; Bozkurt, A.; Yamani, Z. H. Jute Sticks Derived and Commercially Available Activated Carbons for Symmetric Supercapacitors with Bio-Electrolyte: A Comparative Study. *Synthetic Metals*. **2021**, 116765. https://doi.org/10.1016/j.synthmet.2021.116765.

(4) Zequine, C.; Ranaweera, C. K.; Wang, Z.; Dvornic, P. R.; Kahol, P. K.; Singh, S.; Tripathi, P.; Srivastava, O. N.; Singh, S.; Gupta, B. K.; Gupta, G.; Gupta, R. K. High-Performance Flexible Supercapacitors Obtained via Recycled Jute: Bio-Waste to Energy Storage Approach. *Sci. Rep.* **2017**, *7* (1), 1–12. https://doi.org/10.1038/s41598-017-01319-w.

(5) Choi, J.; Wixson, T.; Worsley, A.; Dhungana, S.; Mishra, S. R.; Perez, F.; Gupta, R. K. Pomegranate: An Eco-Friendly Source for Energy Storage Devices. *Surface and Coatings Technology*. **2021**, 127405. https://doi.org/10.1016/j.surfcoat.2021.127405.

(6) Liu, S.; Zhao, Y.; Zhang, B.; Xia, H.; Zhou, J.; Xie, W.; Li, H. Nano-Micro Carbon Spheres Anchored on Porous Carbon Derived from Dual-Biomass as High Rate Performance Supercapacitor Electrodes. *Journal of Power Sources*. **2018**, pp 116–126. https://doi.org/10.1016/j.jpowsour.2018.02.014.

(7) Zhang, H.; Zhou, X. L.; Shao, L. M.; Lü, F.; He, P. J. Hierarchical Porous Carbon Spheres from Low-Density Polyethylene for High-Performance Supercapacitors. *ACS Sustain. Chem. Eng.* **2019**, *7* (4), 3801–3810. https://doi.org/10.1021/acssuschemeng.8b04539.

(8) Zhu, B.; Liu, B.; Qu, C.; Zhang, H.; Guo, W.; Liang, Z.; Chen, F.; Zou, R. Tailoring Biomass-Derived Carbon for High-Performance Supercapacitors from Controllably

Cultivated Algae Microspheres. *J. Mater. Chem. A* **2018**, *6* (4), 1523–1530. https://doi.org/10.1039/c7ta09608a.

(9) Cai, N.; Cheng, H.; Jin, H.; Liu, H.; Zhang, P.; Wang, M. Porous Carbon Derived from Cashew Nut Husk Biomass Waste for High-Performance Supercapacitors. *Journal of Electroanalytical Chemistry*. **2020**, 113933. https://doi.org/10.1016/j.jelechem.2020.113933.

(10) Zhao, Q.; Yang, D.; Zhang, C.; Liu, X. H.; Fan, X.; Whittaker, A. K.; Zhao, X. S. Tailored Polyimide-Graphene Nanocomposite as Negative Electrode and Reduced Graphene Oxide as Positive Electrode for Flexible Hybrid Sodium-Ion Capacitors. *ACS Appl. Mater. Interfaces* **2018**, *10* (50), 43730–43739. https://doi.org/10.1021/acsami.8b17171.

(11) Jayaraman, S.; Jain, A.; Ulaganathan, M.; Edison, E.; Srinivasan, M. P.; Balasubramanian, R.; Aravindan, V.; Madhavi, S. Li-Ion vs. Na-Ion Capacitors: A Performance Evaluation with Coconut Shell Derived Mesoporous Carbon and Natural Plant Based Hard Carbon. *Chemical Engineering Journal*. **2017**, pp 506–513. https://doi.org/10.1016/j.cej.2017.01.108.

(12) Runyu, Yan.; Karen, L.; Jan, P. H.; Markus, A.; Martin, O.; Porous Nitrogen-Doped Carbon/ Carbon Nanocomposite Electrodes Enable Sodium Ion Capacitors with High Capacity and Rate Capability, *Nano Energy*, **2020**, *67*, 104240. https://doi.org/10.1016/j.nanoen.2019.104240.

(13) Xu, J.; Liu, Z.; Zhang, F.; Tao, J.; Shen, L.; Zhang, X. Bacterial Cellulose-Derived Carbon Nanofibers as Both Anode and Cathode for Hybrid Sodium Ion Capacitor. *RSC Adv.* **2020**, *10* (13), 7780–7790. https://doi.org/10.1039/c9ra10225f.

(14) Zhang, H.; Hu, M.; Huang, Z. H.; Kang, F.; Lv, R. Sodium-Ion Capacitors with Superior Energy-Power Performance by Using Carbon-Based Materials in Both Electrodes. *Progress in Natural Science: Materials International*. **2020**, pp 13–19. https://doi.org/10.1016/j.pnsc.2020.01.009.

(15) Wang, S.; Wang, R.; Zhang, Y.; Jin, D.; Zhang, L. Scalable and Sustainable Synthesis of Carbon Microspheres via a Purification-Free Strategy for Sodium-Ion Capacitors. *Journal of Power Sources*. **2018**, pp 33–40. https://doi.org/10.1016/j.jpowsour.2018.01.019.

(16) Yu, Q.; Dong, T.; Qiu, R.; Wang, H. Sulfur and Nitrogen Dual-Doped Carbon Nanofiber with Enlarged Interlayer Distance as a Superior Anode Material for Sodium-Ion Capacitors. *Materials Research Bulletin*. **2021**, 111211. https://doi.org/10.1016/j.materresbull.2021.111211.

(17) Huang, T.; Liu, Z.; Yu, F.; Wang, F.; Li, D.; Fu, L.; Chen, Y.; Wang, H.; Xie, Q.; Yao, S.; Wu, Y. Boosting Capacitive Sodium-Ion Storage in Electrochemically Exfoliated Graphite for Sodium-Ion Capacitors. *ACS Appl. Mater. Interfaces* **2020**, *12* (47), 52635–52642. https://doi.org/10.1021/acsami.0c14611.

(18) Ajuria, J.; Redondo, E.; Arnaiz, M.; Mysyk, R.; Rojo, T.; Goikolea, E. Lithium and Sodium Ion Capacitors with High Energy and Power Densities Based on Carbons from Recycled Olive Pits. *Journal of Power Sources*. **2017**, pp 17–26. https://doi.org/10.1016/j.jpowsour.2017.04.107.

(19) Babu, B.; Ullattil, S. G.; Prasannachandran, R.; Kavil, J.; Periyat, P.; Shaijumon, M. M. Ti3+ Induced Brown TiO2 Nanotubes for High Performance Sodium-Ion Hybrid Capacitors. *ACS Sustain. Chem. Eng.* **2018**, *6* (4), 5401–5412. https://doi.org/10.1021/acssuschemeng.8b00236.

(20) Zhao, N.; Wang, C.; Li, B.; Shen, W.; Kang, F.; Huang, Z. H. Construction of Flexible Lignin/Polyacrylonitrile-Based Carbon Nanofibers for Dual-Carbon Sodium-Ion Capacitors. *J. Mater. Sci.* **2022**, *57* (25), 11809–11823. https://doi.org/10.1007/s10853-022-07371-w.

(21) Jun, Y.; Xiang, H.; Junwei, L.; Yangjie, L.; Guobao, Z.; Taixhing, H. V_2O_3 Nanoparticles Con Fi Ned in High-Conductivity and High- Throughput Carbon Nano Fi Ber Nanohybrids for Advanced Sodium- Ion Capacitors. *ACS Appl. Mater. Interfaces* **2021**, *13*, 10001-10012. https://doi.org/10.1021/acsami.0c21313.